# Carboxyester Hydrolysis Promoted by a New Zinc(II) Macrocyclic Triamine Complex with an Alkoxide Pendant: A Model Study for the Serine Alkoxide Nucleophile in Zinc Enzymes

**Eiichi Kimura,*,† Ikushi Nakamura,† Tohru Koike,† Mitsuhiko Shionoya,† Yorimitsu Kodama,† Takuya Ikeda,† and Motoo Shiro‡**

*Contribution from the Department of Medicinal Chemistry, School of Medicine, Hiroshima University, Kasumi 1-2-3, Minami-ku, Hiroshima 734, Japan, and Rigaku Corporation, Matsubaracho 3-9-12, Akishima, Tokyo 196, Japan*

*Received December 6, 1993⊛*

**Abstract:** New alcohol-pendant 1,5,9-triazacyclododecane ([12]aneN$_3$) ligands, $\mathbf{L_2}$, $\mathbf{L_3}$, and $\mathbf{L_4}$, have been synthesized and characterized. A complexation study on the $Zn^{II}$ complexes of these macrocyclic polyamines has revealed that the pendant alcohol of **9** ($Zn^{II}\mathbf{L_2}$) deprotonates with an extremely low p$K_a$ value of 7.4 at 25 °C to become an alkoxide anion donor at the fourth coordination site. This is a novel chemical illustration that the serine residue located at the center of zinc enzymes can be deprotonated at physiological pH. The alkoxide-coordinating complex **10** was crystallized as the dimeric complex **17** from an aqueous solution of $\mathbf{L_2}$ and $Zn(ClO_4)_2$ at pH 9. The X-ray study of **17** shows each $Zn^{II}$ ion to be 5-coordinate with a short intramolecular $Zn^{II}$–$O^-$(alkoxide) bond (1.950(6) Å) and a relatively longer intermolecular $Zn^{II}$–$O^-$(alkoxide) bond (2.079(5) Å). Crystals of **17**·$(ClO_4)_2$ ($C_{11}H_{24}N_3O_5ClZn$ determined as the monomer) are monoclinic, space group $P2_1/n$ with $a$ = 8.655(1) Å, $b$ = 19.874(1) Å, $c$ = 9.351(2) Å, $\beta$ = 95.90(1)°, $V$ = 1600(4) Å$^3$, and $Z$ = 4. A full-matrix least-squares refinement yielded $R$ = 0.071 and $R_w$ = 0.099 for 1765 independent reflections. In $CH_3CN$ solution, the main species is the dimer **17**, whereas in aqueous solution, it is the monomer **10**, as found by NMR and potentiometric pH titration studies. The $Zn^{II}$-bound alkoxide of **10** is shown to be a very reactive nucleophile and catalyzes 4-nitrophenyl acetate (NA) hydrolysis. A kinetic study of NA hydrolysis by **10** in 10% (v/v) $CH_3CN$ at 25 °C, $I$ = 0.10 ($NaNO_3$), and pH 9.3 (20 mM CHES buffer), has established a second-order rate constant of 1.4 × $10^{-1}$ $M^{-1}$ $s^{-1}$, which is almost 4 times greater than the corresponding value of 3.6 × $10^{-2}$ $M^{-1}$ $s^{-1}$ for the $Zn^{II}$ [12]aneN$_3$ complex **7**. Thus, our present model study shows for the first time that the $Zn^{II}$-bound alkoxide is a better nucleophile than the $Zn^{II}$-bound hydroxide. Moreover, in the course of NA hydrolysis by **10**, we have observed the occurrence of a transient acetyl group transfer from the substrate NA to the pendant alkoxide to yield the O-acetylated species **23**, which was very rapidly hydrolyzed at alkaline pH. The intermediate **23** was independently isolated from the reaction in $CH_3CN$ solution and fully identified as the $Zn^{II}$-free ligand **24**. The mechanism of catalysis by **10** is compared to the one already proposed for serine-containing enzymes (e.g., hydrolytic serine enzymes and alkaline phosphatase).

## Introduction

Alkaline phosphatase (AP) is a $Zn^{II}$-containing phosphomonoesterase that hydrolyzes phosphate monoesters ($ROPO_3^{2-}$) at alkaline pH.[1] Serine(102) under the effect of the $Zn^{II}$ at the AP active center **1** is directly involved in the phosphate hydrolysis.[2] On the basis of X-ray structure[3] and NMR studies,[4] it is now considered that the phosphate substrate is initially attacked by the deprotonated serine(102) to yield a transient phosphoseryl intermediate **2**, which is then attacked intramolecularly by the adjacent $Zn^{II}$-bound hydroxide to complete the hydrolysis and reproduce the free form of serine(102) to reinitiate the catalytic cycle (see **3** in Scheme 1). There are some interesting questions which arise concerning this mechanism, such as: (i) How does the serine(102) hydroxyl group associated with the $Zn^{II}$ ion become a nucleophile? and (ii) What is the special chemical advantage in forming the phosphoseryl intermediate **2** for indirect hydrolysis? In other hydrolytic $Zn^{II}$ enzymes, direct hydrolysis by $Zn^{II}$–$OH^-$ species is prevalent (e.g., aromatic ester hydrolysis by carbonic anhydrase).[5]

There have been numerous reports of phosphate esterase model systems using metal complexes, but most of these models have

**Scheme 1**

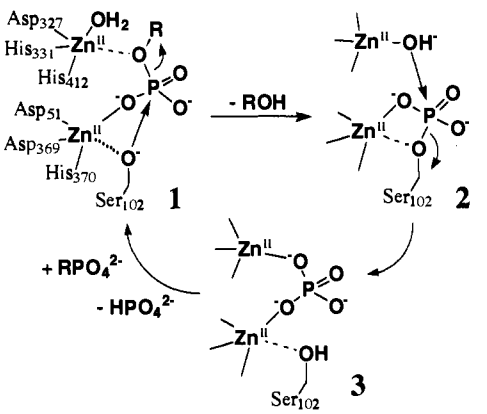


† Hiroshima University.
‡ Rigaku Corporation.
⊛ Abstract published in *Advance ACS Abstracts*, May 1, 1994.

(1) (a) Plocke, D. J.; Levinthal, C.; Vallee, B. L. *Biochemistry* **1962**, *1*, 373. (b) Coleman, J. E. *Annu. Rev. Biophys. Biomol. Struct.* **1992**, *21*, 441.

(2) (a) Butler-Ransohoff, J. E.; Kendall, D. A.; Kaiser, E. T. *Metal ions in biological systems*; Marcel Dekker: New York, 1989; Vol. 25, Chapter 11, p 395. (b) Coleman, J. E.; Besman, M. J. A. *Hydrolytic Enzymes*; Elsevier Science: Amsterdam, 1987; Chapter 8, p 377. (c) Butler-Randohoff, J. E.; Rokita, S. E.; Kendall, D. A.; Banzon, J. A.; Carano, K. S.; Kaiser, E. T.; Martlin, A. R. *J. Org. Chem.* **1992**, *57*, 142.

(3) Kim, E. E.; Wyckoff, H. W. *J. Mol. Biol.* **1991**, *218*, 449.

(4) (a) Gettins, P.; Coleman, J. E. *J. Biol. Chem.* **1984**, *259*, 4991. (b) Hull, W. E.; Halford, S. E.; Gutfreund, H.; Sykes, B. D. *Biochemistry* **1976**, *15*, 1547. (c) Bock, J. L.; Cohn, M. *J. Biol. Chem.* **1978**, *253*, 4082. (d) Coleman, J. E.; Gettins, P. *Zinc Enzymes*; Birkhäuser: Boston, 1986; Chapter 6, p 77.

0002-7863/94/1516-4764$04.50/0 

**Scheme 2**

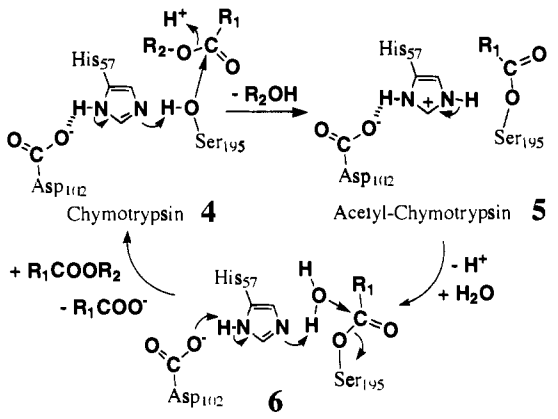


been addressed only to attaining faster hydrolysis rates, and as yet, few systematical models concentrating on the nature of the $Zn^{II}$–serine alkoxide have been given.[6] In 1972, Sigman used a ternary $Zn^{II}$ complex of *N*-(β-hydroxyethyl)ethylenediamine and 4-nitrophenyl picolinate as a catalytic model for $Zn^{II}$–alkoxide-promoted transesterification.[7] Although this model drew some intriguing and convincing pictures about the essential role of the $Zn^{II}$ ion in $Zn^{II}$-containing serine enzymes, there were some limitations to this study, such as: (i) the stoichiometry of the possible reactive $Zn^{II}$-bound alkoxide complex (its estimated $pK_a$ was 8.4) was only kinetically determined; (ii) the ternary complex and the other $Zn^{II}$-bound alkoxide species were not separated and characterized; and (iii) $Zn^{II}$ only catalyzed the transesterification to give the picolinoyl ester of *N*-(β-hydroxyethyl)ethylenediamine, and its subsequent hydrolysis, which is another essential step in serine enzyme reactions, was not possible.

Therefore, the above-mentioned questions still need to be addressed using a more concrete model, since this might add to the fundamental mechanistic knowledge surrounding general "serine proteases" in which the serine OH group is the initial nucleophile and $OH^-$ (or activated $H_2O$) is the second nucleophile. Also, a major difference between alkaline phosphatase and nonmetallic "serine proteases" is that in the latter case, the serine OH group is activated by a base of an adjacent histidyl imidazole, which in turn is linked to a carboxylate anion (see Scheme 2 for chymotrypsin).[8] Therefore, it begs the question why nature adopts $Zn^{II}$ in some cases and imidazole in other cases to make the serine hydroxyl group a strong nucleophile toward electrophilic substrates.

Recently, we discovered that the macrocyclic triamine ([12]-aneN$_3$, **L$_1$**) and tetraamine ([12]aneN$_4$, cyclen)$Zn^{II}$ complexes, **7** and **8**, are good models for the $Zn^{II}$–$OH^-$ nucleophile in hydrolytic $Zn^{II}$ enzymes, carbonic anhydrase[9] and phosphatases.[10] In these complexes, $Zn^{II}$-bound $OH^-$ groups, which are easily generated at physiological pH with $pK_a$ values of 7.3 and 7.9 from the $Zn^{II}$-bound $H_2O$, act as nucleophiles at the electrophilic centers of the substrates. In carbonic anhydrase, the $Zn^{II}$ at the active center is surrounded by three imidazole nitrogens and a water bound at the fourth coordination site which deprotonates at pH ca. 7.[11] In the present study to elucidate the alkaline phosphatase mechanism, we have designed new [12]aneN$_3$ analogues **L$_2$**, **L$_3$**, and **L$_4$** bearing an alcohol pendant. We hoped

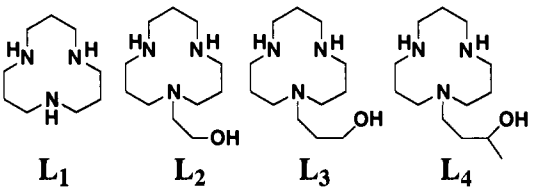


to see whether each pendant alcohol, under the strong influence of the nearby $Zn^{II}$ trapped in the macrocyclic ring, could be deprotonated to become a strong nucleophile and so act as the catalytic site in a similar fashion to the $Zn^{II}$-activated serine OH group in alkaline phosphatase. Indeed, we have discovered that **L$_2$** yields a 1:1 $Zn^{II}$ complex **9**, where the alcoholic OH deprotonates at physiological pH to form **10**. Furthermore, the $Zn^{II}$-bound alkoxide anion in **10** is a stronger nucleophile than the $Zn^{II}$-bound $OH^-$ anion in **7**. We herein describe a novel chemical model for $Zn^{II}$-involving serine enzymes as part of our series of studies on the intrinsic chemical properties of $Zn^{II}$ in biological systems.[12]

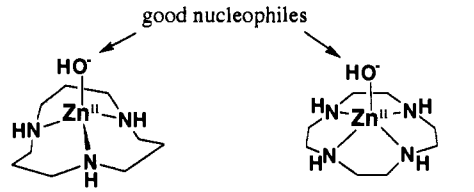


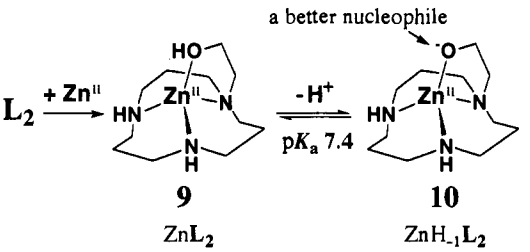


## Results and Discussion

**Syntheses of Alcohol-Pendant [12]aneN$_3$ Ligands, L$_2$, L$_3$, and L$_4$.** Macrocyclic dioxotriamine **11**[13] was treated with ethyl bromoacetate in the presence of an equimolar amount of

(5) (a) Coleman, J. E. *Zinc Enzymes*; Birkhäuser: Boston, 1986; Chapter 4, p 49. (b) In addition to phosphate hydrolysis, alkaline phosphatase catalyzes transesterification of phosphomonoesters if an alcoholic acceptor is present at a sufficiently high concentration. The phosphoseryl intermediate **2** might undergo transesterification to produce an appropriate phosphomonoester without any loss of energy. See: Gettins, P.; Metzler, M.; Coleman, J. E. *J. Biol. Chem.* **1985**, *260*, 2875.

(6) (a) Hendry, P.; Sargeson, A. M. *Progress in Inorganic Chemistry: Bioinorganic Chemistry*; John Wiley & Sons: New York, 1990; Vol. 38, p 201. (b) Hay, R. W. *J. Chem. Soc., Chem. Commun.* **1990**, 714. (c) Morrow, J. R.; Buttrey, L. A.; Berback, K. A. *Inorg. Chem.* **1992**, *31*, 16. (d) Clewley, R. W.; Slebocka-Tilk, H.; Brown, R. S. *Inorg. Chem. Acta* **1989**, *157*, 233. (e) Rosch, M. A. D.; Trogler, W. C. *Inorg. Chem.* **1990**, *29*, 2409. (f) Norman, P. R.; Cornelius, R. D. *J. Am. Chem. Soc.* **1982**, *104*, 2356. (g) Gellman, S. H.; Petter, R.; Breslow, R. *J. Am. Chem. Soc.* **1986**, *108*, 2388. (h) Browne, K.; Bruice, T. C. *J. Am. Chem. Soc.* **1992**, *114*, 4951. (i) Kim, J. H.; Chin, J. *J. Am. Chem. Soc.* **1992**, *114*, 9792. (j) Jones, D. R.; Lindoy, L. F.; Sargeson, *J. Am. Chem. Soc.* **1984**, *106*, 7807. (k) Herschlag, D.; Jencks, W. P. *J. Am. Chem. Soc.* **1987**, *109*, 4665.

(7) Sigman, D. S.; Jorgensen, C. T. *J. Am. Chem. Soc.* **1972**, *94*, 1724.

(8) (a) Blow, D. M.; Birktoft, J. J.; Hartley, B. S. *Nature* **1969**, *221*, 337. (b) Dugas, H. *Bioorganic Chemistry*; Springer-Verlag: New York, 1989; p 196. (c) Polgár, L. *Hydrolytic Enzymes*; Elsevier Science: Amsterdam, 1987; Chapter 3, p 159.

(9) (a) Kimura, E.; Shiota, T.; Koike, T.; Shiro, M.; Kodama, M. *J. Am. Chem. Soc.* **1990**, *112*, 5805. (b) Kimura, E.; Koike, T. *Comments Inorg. Chem.* **1991**, *11*, 285.

(10) Koike, T.; Kimura, E. *J. Am. Chem. Soc.* **1991**, *113*, 8935.

(11) (a) Pocker, Y.; Miao, C. H. *Zinc Enzymes*; Birkhäuser: Boston, 1986; Chapter 25, p 341. (b) Eriksson, A. E.; Kylsten, P. M.; Jones, T. A.; Liljas, A. *Proteins* **1988**, 283.

(12) (a) Shionoya, M.; Kimura, E.; Shiro, M. *J. Am. Chem. Soc.* **1993**, *115*, 6730. (b) Kimura, E.; Shionoya, M.; Hoshino, A.; Ikeda, T.; Yamada, Y. *J. Am. Chem. Soc.* **1992**, *114*, 10134. (c) Kimura, E.; Koike, T.; Shiota, T.; Iitaka, Y. *Inorg. Chem.* **1990**, *29*, 4621.

(13) Helps, I. M.; Parker, D.; Jankowski, K. J.; Chapaman, J.; Nicholson, P. E. *J. Chem. Soc., Perkin Trans. 1* **1989**, 2079.

Table 1. Comparison of the Protonation Constants of $L_1$–$L_4$ and the $Zn^{II}$ Complexation Constants of $L_1$ and $L_2$[a]

| | | $L_2$ | | | | |
|---|---|---|---|---|---|---|
| | $L_1$[b] | 15 °C | 25 °C | 35 °C | $L_3$[c] | $L_4$[c] |
| log $K_1$ | 12.6 | 12.0 ± 0.1 | 11.7 ± 0.1 | 11.3 ± 0.1 | 12.0 ± 0.2 | 12.2 ± 0.2 |
| log $K_2$ | 7.57 | 7.19 ± 0.02 | 6.92 ± 0.02 | 6.65 ± 0.02 | 6.78 ± 0.02 | 6.90 ± 0.02 |
| log $K_3$ | 2.4 | 2.3 ± 0.1 | 2.2 ± 0.1 | 2.0 ± 0.1 | 2.7 ± 0.1 | 2.6 ± 0.1 |
| log $K$(ZnL) | 8.4 | 7.8 ± 0.1 | 7.6 ± 0.1 | 7.3 ± 0.1 | | |
| p$K_a$ | 7.3 | 7.7 ± 0.1 | 7.4 ± 0.1 | 7.1 ± 0.1 | | |
| log $K_d$ | | 1.0 ± 0.3 | 0.8 ± 0.3 | <0 | | |

[a] $K_n = [H_nL]/[H_{n-1}L]a_{H^+}$. $K(ZnL) = [ZnL]/[L][Zn^{II}]$. $K_a = [ZnH_{-1}L]a_{H^+}/[ZnL]$. $K_d = [(ZnH_{-1}L)_2]/[ZnH_{-1}L]^2$. At $I = 0.10$ ($NaNO_3$). [b] From ref 9a at $I = 0.20$ ($NaClO_4$) and 25 °C. [c] At $I = 0.10$ ($NaNO_3$) and 25 °C.

**Scheme 3**

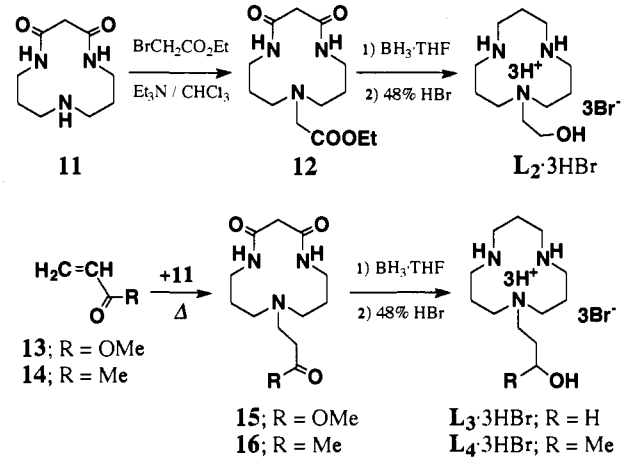


triethylamine in $CHCl_3$ at 50 °C for 1 h to obtain **12** in 61% yield (Scheme 3). All the carbonyl groups were reduced with freshly distilled $BH_3$·THF complex[14] in THF to give the desired product $L_2$, which was purified as its crystalline 3HBr salt in 58% yield.

For $L_3$ and $L_4$, Michael addition reactions were employed. Methyl acrylate **13** and methyl vinyl ketone **14** were reacted with **11** to yield **15** and **16** in 83 and 87% yield, respectively. The following $BH_3$·THF reduction and acidification by 48% aqueous HBr produced the desired products $L_3$ and $L_4$ as crystalline 3HBr salts in 24 and 56% yield, respectively.

**Protonation and Zinc(II) Complexation Constants of $L_2$, $L_3$, and $L_4$.** The protonation constants ($K_n$) of $L_2$, $L_3$, and $L_4$ were determined by potentiometric pH titrations of L·3HBr (1 mM) with 0.10 M NaOH at $I = 0.10$ ($NaNO_3$). A typical pH titration curve for $L_2$·3HBr at 25 °C is shown in Figure 1a. The titration data were analyzed for equilibria 1–3. The mixed protonation constants $K_1$–$K_3$ ($a_{H^+}$ is the activity of $H^+$) are defined as follows:

$$L + H^+ \rightleftharpoons HL \qquad K_1 = [HL]/[L]a_{H^+} \quad (1)$$

$$HL + H^+ \rightleftharpoons H_2L \qquad K_2 = [H_2L]/[HL]a_{H^+} \quad (2)$$

$$H_2L + H^+ \rightleftharpoons H_3L \qquad K_3 = [H_3L]/[H_2L]a_{H^+} \quad (3)$$

Table 1 summarizes the obtained protonation constants (log $K_n$) in comparison with the reported $K_n$ values of [12]aneN$_3$ ($L_1$).[9a] Among the alcohol-pendant ligands $L_2$, $L_3$, and $L_4$, the protonation constants $K_1$–$K_3$ at 25 °C are almost the same. The pendants all act to lower the ligand basicity, as indicated by the smaller $K_1$ and $K_2$ values.

The titration curve of $L_2$·3HBr in the presence of equimolar $Zn^{II}$ (Figure 1b) reveals complex formation at $6 < pH < 9$, with almost simultaneous deprotonation of the pendant alcohol OH, owing to the observation of the sole neutralization break at $a = 4$. The titration data were treated for the 1:1 $Zn^{II}$ complex ZnL

(14) Kimura, E.; Kotake, Y.; Koike, T.; Shionoya, M.; Shiro, M. *Inorg. Chem.* **1990**, *29*, 4991.

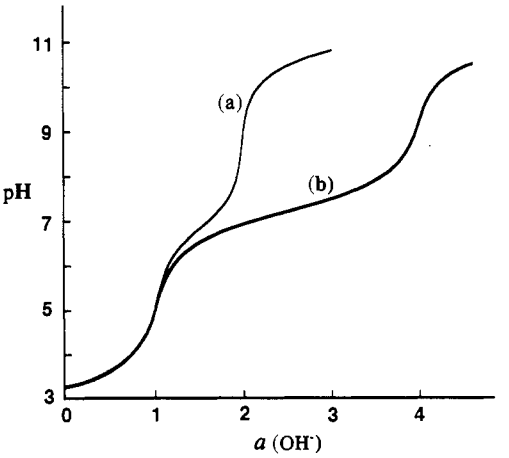


**Figure 1.** Typical titration curves for $L_2$·3HBr at 25 °C and $I = 0.10$ ($NaNO_3$). (a) 1.0 mM $L_2$·3HBr; (b) 1.0 mM $L_2$·3HBr + 1.0 mM $Zn^{II}SO_4$.

(eq 4), its monodeprotonated complex $ZnH_{-1}L$ (eq 5), and the dimeric form of $(ZnH_{-1}L)_2$ (eq 6), where $H_{-1}L$ is an alcoholic OH deprotonated ligand. The conclusive structure assignment for **10** (L = $L_2$) and the dimer **17** comes from the following X-ray crystal analysis and NMR study. The $Zn^{II}$ complexation constants $K$(ZnL), $K_a$ and $K_d$ are defined as follows:

$$L + Zn^{II} \rightleftharpoons ZnL\ (9) \qquad K(ZnL) = [ZnL]/[L][Zn^{II}] \quad (4)$$

$$ZnL \rightleftharpoons ZnH_{-1}L\ (10) + H^+ \qquad K_a = [ZnH_{-1}L]a_{H^+}/[ZnL] \quad (5)$$

$$2ZnH_{-1}L \rightleftharpoons (ZnH_{-1}L)_2\ (17)$$

$$K_d = [(ZnH_{-1}L)_2]/[ZnH_{-1}L]^2 \quad (6)$$

The obtained values for log $K$(ZnL) and the pendant alcohol OH deprotonation constant p$K_a$ at 15, 25, and 35 °C are included in Table 1. A typical diagram for species distribution as a function

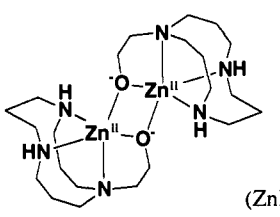


**17**
$(ZnH_{-1}L_2)_2$

of −log [$H^+$] at [total zinc] = [total $L_2$] = 1 mM and 25 °C is displayed in Figure 2. *The most significant finding is the extremely facile deprotonation of the alcoholic OH with p$K_a$ values of 7.7 (15 °C), 7.4 (25 °C), and 7.1 (35 °C) at the fourth coordination site of the $Zn^{II}$.* It is of interest to note that the water at the fourth coordination site of $Zn^{II}$ [12]aneN$_3$ deprotonates to give **7** with a similar p$K_a$ of 7.3 at 25 °C.[9a] Moreover, the obtained dimerization constants ($M^{-1}$) of 1.0 ± 0.3 (15 °C),

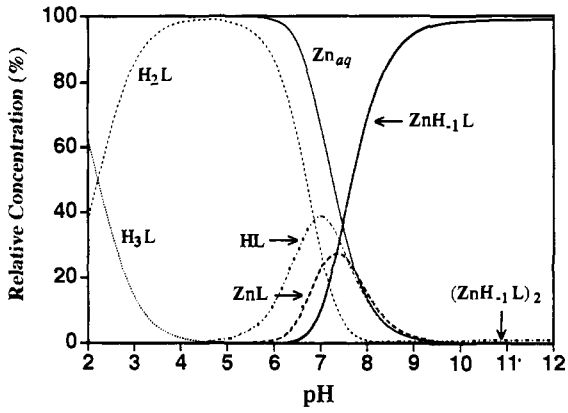


**Figure 2.** Distribution diagram for 1 mM $Zn^{II}$/1 mM $L_2$ system as a function of pH at 25 °C and $I$ = 0.10 ($NaNO_3$). $(ZnH_{-1}L)_2$ is the dimeric complex **17**; $ZnH_{-1}L$ is the monomeric complex **10**; ZnL is **9**.

0.8 ± 0.3 (25 °C), and <0 (35 °C) are so small that more than 98% of total zinc species is monomeric complex **10** at [total zinc complex] = ca. 1 mM in aqueous solution (see Figure 2). The present new complex **10** may therefore serve as a good model to illustrate the ability of $Zn^{II}$ to deprotonate the serine hydroxyl group at the active center of alkaline phosphatase.

In a similar manner, the $Zn^{II}$ complexations of $L_3$ and $L_4$ were studied. However, a higher pH (e.g., pH value was ca. 8 ($a$ = 2.5) at [total zinc] = [total ligand] = 1 mM) was required for $Zn^{II}$ complexation to occur, which clearly indicates that ZnL for $L_3$ and $L_4$ is less stable than for $L_2$. Furthermore, at pH > ca. 8, partial decomposition (due to $Zn(OH)_2$ formation) occurred before the deprotonation of the pendant propyl alcohol could compete. We thus failed to determine the $Zn^{II}$ complexation constants using the pH titration data. The ligand $K_n$ values are shown in Table 1. Initially, we thought that the $Zn^{II}$ complexes of the propanol-pendant ligands $L_3$ and $L_4$ might be more stable than the $L_2$ complex, since computer graphic modeling studies suggested that the $Zn^{II}$ complexes with $L_3$ and $L_4$ appeared to form an ideal tetrahedral structure **18** due to the 6-membered ($Zn^{II}$-N-$C_3$-O$^-$-($Zn^{II}$)) chelate ring. Previously, it was shown that a propylene chain enables an anionic N$^-$ donor to be located at the apex of tetrahedral position by an X-ray structure of the sulfonamidopropyl-pendant [12]ane$N_3$ complex **19**.[15] However, the ethylene chain in $L_2$ yields a more stable complex than the propylene chains in $L_3$ and $L_4$. This seems to support the theory that the $Zn^{II}$ in [12]ane$N_3$ prefers to bind an anionic donor at the equatorial position of a 5-coordinate trigonal-bipyramidal complex **20** (short equatorial and long axial coordinate bonds) rather than as a 4-coordinate tetrahedron. Indeed, the following X-ray structure of the dimeric $Zn^{II}$ complex **17** agrees with this notion. A similar coordination mode was also seen with the X-ray crystal structures of the phenolate-pendant [12]ane$N_3$ $Zn^{II}$ complex **21**[16] and the $Zn^{II}$ [12]ane$N_3$ dithiocyanate complex **22**.[17]

**X-ray Crystal Structure of the Dimeric Form 17 of $ZnH_{-1}L_2$ (10).** A solution of $Zn^{II}(ClO_4)_2 \cdot 6H_2O$ was added to $L_2 \cdot 3HBr$ in $H_2O$, and the solution pH was adjusted to 9 with 1 M NaOH aqueous solution, where the deprotonated complex $ZnH_{-1}L_2$ **10** was found to be the predominant species in solution from the above pH titration study. After addition of an excess amount of $NaClO_4$, colorless crystals were collected. The elemental analysis (C, H, N) and IR data suggested the formula $ZnH_{-1}L_2 \cdot ClO_4$. The ultimate support for the alkoxide-coordinating dimeric structure **17** with two perchlorates comes from the resulting X-ray crystal structure analysis. Figure 3 shows an ORTEP drawing

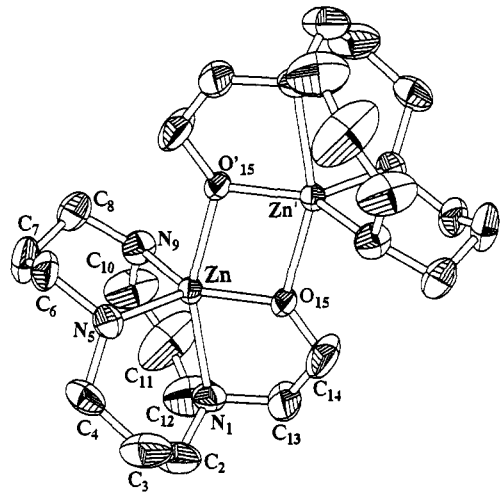


**Figure 3.** ORTEP drawing (30% probability thermal ellipsoids) of **17**·$(ClO_4)_2$. All hydrogen atoms and two perchlorate anions are omitted for clarity.

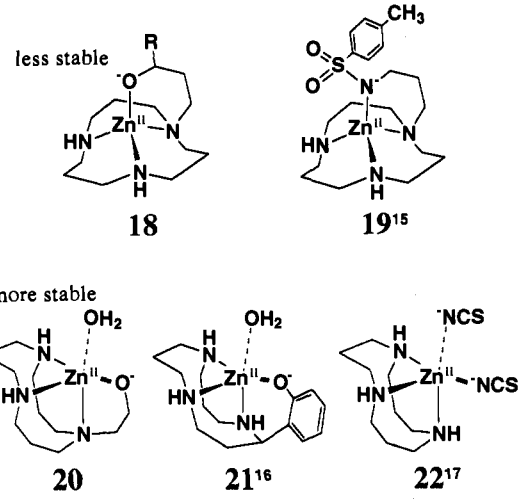


of the cationic part of the dimeric complex with 30% probability thermal ellipsoids. Crystal data and data collection parameters are displayed in Table 2. Selected bond distances and bond angles around $Zn^{II}$ are given in Table 3.

In the dimeric complex **17**, there are two $[ZnH_{-1}L_2]^+$ ions around a crystallographic 2-fold axis. Each $Zn^{II}$ is surrounded in a distorted trigonal-bipyramidal environment by the three N atoms ($N_1$, $N_5$, $N_9$) of the macrocyclic ligand, the internal pendant oxygen ($O_{15}$), and the external pendant oxygen ($O'_{15}$) of the adjacent complex. The zinc atom lies almost in the basal plane defined by the $N_5$, $N_9$, and alkoxide $O_{15}$ atoms with a total angle of 359.9° for $N_5$–Zn–$N_9$, $N_9$–Zn–$O_{15}$, and $O_{15}$–Zn–$N_5$. The apical angle $N_1$–Zn–$O'_{15}$ is bent at 161.1°. The present 5-coordinate structure may be compared with the previous 4-coordinate (tetrahedral) structure of the tosylamidopropyl-[12]ane$N_3$ $Zn^{II}$ complex, **19**.[15] In **17**, the Zn–$O_{15}$ bond (1.950 Å) is shortened at the expense of an elongated bond of the Zn–$N_1$ (2.259 Å), whereas in the tetrahedral **19**, the Zn–N$^-$ (1.925 Å) is shorter and the Zn–$N_1$ (2.037 Å) is almost the same length as the other Zn–secondary N bonds (2.019 and 2.018 Å). This difference is probably due to the shorter arm span for the ethylene bridge in **17**. The somewhat strained $N_3O^-$ coordination in **17** is balanced by the additional O$^-$ coordination from an adjacent external ethoxide $O'_{15}$. The strong $Zn^{II}$–O$^-$ intramolecular binding is the reason for the extremely low p$K_a$ value of 7.4 for $NCH_2CH_2OH$ in **9** ⇌ $NCH_2CH_2O^-$ in **10**, which is almost $10^8$ times lower than that for the metal-unbound alcohol.

**Solution Structure Studies of 10 (or 20) and 17.** To determine whether the equilibrium between monomer **10** (or **20**) and dimer

(15) Koike, T.; Kimura, E.; Nakamura, I.; Hashimoto, Y.; Shiro, M. *J. Am. Chem. Soc.* **1992**, *114*, 7338.
(16) Kimura, E.; Koike, T.; Toriumi, K. *Inorg. Chem.* **1988**, *27*, 3687.
(17) Kimura, E.; Koike, T.; Shionoya, M.; Shiro, M. *Chem. Lett.* **1992**, 787.

**Table 2.** Crystallographic Parameters for the Monomeric Part of **17**·$(ClO_4)_2$

| | |
|---|---|
| formula | $C_{11}H_{24}N_3O_5ClZn$ |
| formula weight | 379.16 |
| cryst syst | monoclinic |
| space group | $P2_1/n$ (No. 14) |
| cryst color | colorless |
| cell dimens | |
| $a$, Å | 8.655(1) |
| $b$, Å | 19.874(1) |
| $c$, Å | 9.351(2) |
| $\beta$, deg | 95.90(1) |
| $V$, Å$^3$ | 1600.0(4) |
| $Z$ | 4 |
| $d_{calcd}$, g cm$^{-3}$ | 1.574 |
| cryst dimers, mm | 0.2 × 0.15 × 0.05 |
| radiation | Cu K$\alpha$ ($\lambda$ = 1.541 78 Å) |
| $\mu$, cm$^{-1}$ | 39.48 |
| temp, K | 296 ± 1 |
| scan technique | $\omega - 2\theta$ |
| scan width, det | 1.73 + 0.30 tan $\theta$ |
| scan speed, deg min$^{-1}$ | 16.0 (in $\omega$) |
| refinement | full-matrix least-squares |
| no. unique reflcns | 2470 |
| no. obsd reflcns ($I < 3\sigma(I)$) | 1765 |
| $R$ | 0.071 |
| $R_w$ | 0.099 |

**Table 3.** Selected Bond Distances and Bond Angles for **17**·$(ClO_4)_2$

| | | | |
|---|---|---|---|
| | Bond Distances (Å) | | |
| Zn–N(1) | 2.259(8) | Zn–N(5) | 2.047(7) |
| Zn–N(9) | 2.067(8) | Zn–O(15) | 1.950(6) |
| Zn–O(15′) | 2.079(5) | | |
| | Bond Angles (deg) | | |
| O(15)–Zn–O(15′) | 78.3(3) | O(15)–Zn–N(1) | 82.8(3) |
| O(15)–Zn–N(5) | 126.8(3) | O(15)–Zn–N(9) | 94.9(3) |
| O(15′)–Zn–N(1) | 161.1(3) | O(15′)–Zn–N(5) | 95.9(3) |
| O(15′)–Zn–N(9) | 94.9(3) | N(1)–Zn–N(5) | 95.8(3) |
| N(1)–Zn–N(9) | 97.1(3) | N(5)–Zn–N(9) | 102.3(3) |

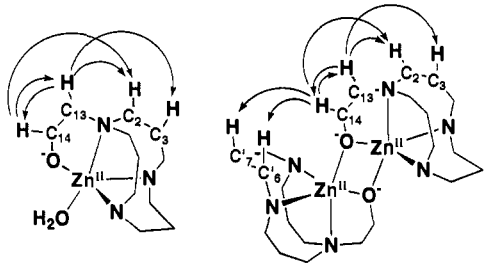

**20** in $D_2O$ **17** in $CD_3CN$

**Figure 4.** Proposed main structures of **20** in $D_2O$ and **17** in $CD_3CN$ with the observed NOE correlations upon irradiation of $H(C_{13})$ or $H(C_{14})$ at [total $Zn^{II}$] = 20 mM and 30 °C. **20**, $HC_{14}$→$HC_{13}$ 10.3%, $HC_{14}$→$HC_2$ 2.6%, $HC_{13}$→$HC_{14}$ 9.8%, $HC_{13}$→$HC_2$ 6.2%, $HC_{13}$→$HC_3$ 4.7%; **17**, $HC_{14}$→$HC_{13}$ 9.7%, $HC_{14}$→$HC_2$ 4.5%, $HC_{14}$→$HC'_7$ 1.2%, $HC_{14}$→$HC'_6$ 5.3%, $HC_{13}$→$HC_{14}$ 9.2%, $HC_{13}$→$HC_2$ 6.2%, $HC_{13}$→$HC_3$ 4.1%.

**17** occurs in solution, we have measured the NMR chemical shifts for all the methylene protons and the coupling patterns at a higher concentration ([total zinc] = [total ligand] = 20 mM) than that used for the potentiometric pH titrations. The $^1H$ NMR peak assignments were made with the assistance of COSY and NOE (upon irradiation of $H(C_{13})$ or $H(C_{14})$, [total zinc] = [total ligand] = 20 mM) experiments (see Figure 4). Over a range of 0.5–20 mM concentration of total $Zn^{II}$ in the presence of equimolar $L_2$ in $D_2O$ solution (pD 9.5), the $^1H$ signals did not shift at all at 30 °C, and the proton coupling correlations did not change between 25 and 40 °C. Typical coupling constants and chemical shifts at 30 °C are shown in the Experimental Section. NOEs

**Scheme 4**

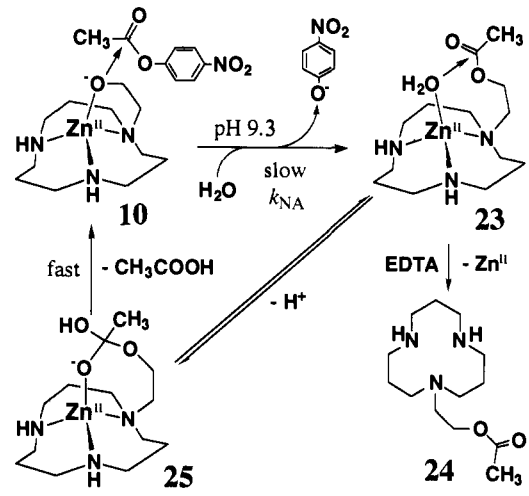


expected on the basis of intramolecular cross-relaxation for $H(C_{13})$ and $H(C_{14})$ were seen in $D_2O$ at 30 °C. However, no NOE derived from intermolecular cross-relaxation was observed. These results are in agreement with the monomeric structure of $ZnH_{-1}L_2$ **10** (or **20**) in aqueous solution, which also conforms to the result from the above potentiometric pH titrations.

On the other hand, the NMR chemical shifts and the coupling patterns of **17** in $CD_3CN$ were different from those in $D_2O$ (see the Experimental Section). Furthermore, two intermolecular NOEs for $H(C_{14})$→$H(C'_7)$ and $H(C_{14})$→$H(C'_6)$ were observed along with the expected intramolecular NOEs upon irradiation of $H(C_{14})$ at [total zinc] = [total ligand] = 20 mM (see Figure 4). The intermolecular cross-relaxations strongly suggest that the dimeric structure **17** is present in $CD_3CN$. Moreover, these NOE signals completely vanished in the presence of 50% (v/v) $D_2O$. This can be explained by the fact that the dimeric structure **17** is decomposed by hydration and/or water coordination at the fifth coordination site (see **20**).

Next, the conductance of $ZnH_{-1}L_2$·$ClO_4$ was measured in 0.1 M CHES buffer (pH 9.1) at 37 °C in the total zinc concentration range of 0.63–10 mM. The conductance changes linearly with concentration, and no deviation from the line was observed. The calculated relative conductance value of 60 ± 3 $\Omega^{-1}$ cm$^2$ mol$^{-1}$ for $(ZnH_{-1}L_2)ClO_4$ is almost identical to that of 63 ± 3 $\Omega^{-1}$ cm$^2$ mol$^{-1}$ for $(ZnL_1OH)ClO_4$ (measured under the same conditions). These results give further support for the monomeric structure **10** (or **20**) in aqueous solution, and therefore this monomeric structural assignment was adopted for the kinetic studies described below.

**4-Nitrophenyl Acetate (NA) Hydrolysis by 10.** The $ZnH_{-1}L_2$ complex **10** was next tested as a model for one of the $Zn^{II}$ sites in alkaline phosphatase. Since the phosphomonoesters (e.g., 4-nitrophenyl phosphate) underwent extremely slow hydrolysis with **10**, we turned to carboxyester 4-nitrophenyl acetate (NA) hydrolysis promoted by **10** at pH 9.5 (15 °C), 9.3 (25 °C), and 9.1 (35 °C) (20 mM CHES buffer, where the complex is almost exclusively in the form of $ZnH_{-1}L_2$, $I$ = 0.10 ($NaNO_3$)) in 10% (v/v) $CH_3CN$ aqueous solution (see Scheme 4). The hydrolysis was followed by the appearance of the 4-nitrophenolate anion at 400 nm. The second-order dependence of the rate constant on the total concentration of $Zn^{II}$ complex (0.5–3 mM calculated as the monomeric form) and [NA] (0.1, 0.5, 1.0, and 2.0 mM) is consistent with catalysis by the monomeric complex **10**. Previously,[9,10] NA hydrolysis catalyzed by **7** and **8** was measured by a similar method at 25 °C.

The obtained second-order rate constants $k_{NA}$ of **10** were (0.70 ± 0.04) × $10^{-1}$, (1.4 ± 0.1) × $10^{-1}$, and (2.8 ± 0.1) × $10^{-1}$ M$^{-1}$ s$^{-1}$ at 15, 25, and 35 °C, respectively. These $k_{NA}$ values did not significantly change (within 10%) when $D_2O$ solution (10% (v/

v) $CH_3CN$) was used. This small isotope effect implies that the $Zn^{II}$-bound alkoxide acts directly as a nucleophile toward NA and not as a base catalyst producing an aqueous hydroxide anion. The activation energy $E_a$ for the nucleophilic attack of **10** is calculated to be 51 ± 2 kJ $mol^{-1}$, with a frequency factor of 1.2 × $10^8$ $M^{-1}$ $s^{-1}$. Since the initial $k_{NA}$ value holds after more than one catalytic cycle, the hydrolysis by **10** is concluded to be a catalytic reaction (see the Experimental Section).

In the course of the catalytic NA hydrolysis, we suspected that a transient "acetyl intermediate" **23** was formed, which then disappeared very rapidly to give the final product $CH_3COO^-$ and **10** (see Scheme 4 and the Experimental Section). The acetyl intermediate **23** was independently confirmed by isolation of the $Zn^{II}$-free ligand **24** from the reaction of NA with **10** in $CH_3CN$, followed by addition of aqueous EDTA solution and $KPF_6$ to the reaction mixture to give **24** as its $HPF_6$ salt. An $^1H$ NMR study showed that when **24** was dissolved in 10% (v/v) $CD_3CN/D_2O$ solution (pD 9.5, 0.1 M CHES buffer), the acetate moiety was not hydrolyzed, but the subsequent addition of $Zn(ClO_4)_2$ caused prompt hydrolysis to yield $CH_3COO^-$ and **10**. In addition, transient proton signals (δ 2.13 and 4.23, 10 mol % of **10**) assigned to the methyl and pendant methylene protons of **23** were detected ca. 5 min after mixing 16 mM of **10** and 8 mM of NA in 10% (v/v) $CD_3CN/D_2O$ solution (pD 9.2, 0.3 M borate buffer), but these had completely disappeared on reinspection 1 h later. We failed to isolate the $Zn^{II}$-coordinating intermediate complex **23**, probably due to its reactivity and/or instability. These facts indicate that the $Zn^{II}$ in **23** immediately promotes intramolecular ester hydrolysis. Thus, we propose the overall catalytic reaction depicted in Scheme 4, in which the slowest step is the initial formation of **23**. Before any $Zn^{II}$ dissociates from the acetyl intermediate **23** ($Zn^{II}$ is three-coordinate before water binding, and hence would be fairly labile), the $Zn^{II}$–$OH^-$ form is generated by the strong acidity of $Zn^{II}$, which then rapidly attacks the intramolecular acetate carbonyl carbon. The postulated anion-bound intermediate **25** would lower the transition energy and greatly facilitate the ester hydrolysis. Additionally, the regenerated catalyst **10** is greatly stabilized by the strong alkoxide anion coordination.

**NA Hydrolysis: A Comparison between the $Zn^{II}$ Alkoxide in 10 and the $Zn^{II}$ Hydroxide in 7.** Using the same conditions, the second-order rate constants $k_{NA}$ for NA hydrolysis with **7** were determined to be (2.2 ± 0.2) × $10^{-2}$, (3.6 ± 0.3) × $10^{-2}$, and (8.3 ± 0.5) × $10^{-2}$ $M^{-1}$ $s^{-1}$ at pH 9.5 (15 °C), 9.3 (25 °C), and 9.1 (35 °C), respectively. The present kinetic data at 25 °C agree with our previous results.[9a] With the kinetic data for both the $RO^-$–$Zn^{II}$ and the $HO^-$–$Zn^{II}$ nucleophilic reactions in hand, we can conclude that *the $RO^-$–$Zn^{II}$ of **10** is approximately 4 times as strong a nucleophile as the $HO^-$–$Zn^{II}$ of **7** at 25 °C.* Moreover, it is of interest to point out that the basicity of the $RO^-$–$Zn^{II}$ of **10** ($pK_a$ 7.4) and the $HO^-$–$Zn^{II}$ of **7** ($pK_a$ 7.3) are almost the same. To our knowledge, this is the first demonstration that a $Zn^{II}$-bound alkoxide can be a better nucleophile than a $Zn^{II}$-bound hydroxide. This might also be the case in hydrolytic $Zn^{II}$ enzymes, where the majority adopts serine or threonine (or their alkoxides) as strong nucleophiles.[18]

The activation energy $E_a$ of 49 ± 2 kJ $mol^{-1}$ for NA hydrolysis with **7** is similar to that with **10**, but the frequency factor of 1.4 × $10^7$ $M^{-1}$ $s^{-1}$ for **7** is ca. 9 times smaller. With **7**, no isotope effect was observed in $D_2O$ solution (10% (v/v) $CH_3CN$), which indicates that the $Zn^{II}$-bound hydroxide directly attacks NA. Therefore, since $O^-$ anion nucleophilic attack of both **7** and **10** is the rate-determining step, the faster rate with **10** is rationalized by the $RO^-$–$Zn^{II}$ being more naked (less solvated due to steric hindrance from the lipophilic ethylene bridge attached to the $O^-$ anion), whereas the $HO^-$–$Zn^{II}$ of **7** is more tightly solvated by hydrogen bonding, and hence the lone pair directed toward the electrophile (NA) is more shielded.[19] This interpretation also agrees with the larger frequency factor for **10** over **7**.

**Ester Hydrolysis: A Comparison between 10 and Chymotrypsin 4.** In comparing the acyl-transfer reactions of the complex **10** (see Scheme 4) with those of chymotrypsin **4** (see Scheme 2),[8,20] we find that the alcoholic nucleophiles in **10** and **4** are activated by an acid and base, respectively, but both catalytic cycles proceed via a "two-step" (double replacement) process which has several common features. (i) In the first step, the substrate acylates the serine residue in the active site, i.e., the "acylchymotrypsin" **5** is formed which has been unambiguously identified. From the reaction mixture the enzymatically inactive "acylchymotrypsin" **5** can be isolated. By analogy, the *O*-acetyl ligand **24** can be isolated when NA is treated with **10**. (ii) Both the acetyl intermediates are solvolyzed to liberate acetate and regenerate the catalyst. (iii) In the chymotrypsin-catalyzed hydrolysis of nonlabile esters and carboxyamides at physiological pH, a similar "two-step" mechanism holds.[8,20] In these cases, the initial acylation is rate-determining. This situation is somewhat analogous to our reactions. (iv) In NA hydrolysis with chymotrypsin **4**, the pH dependencies of both the acylation and the deacylation step point to the involvement of a general base or nucleophile with a kinetically revealed $pK_a$ value of approximately 7, which is somewhat analogous to the $pK_a$ value of 7.4 for **10**. If a mechanism involving only the imidazole as a general base is assumed, this $pK_a$ probably denotes the acidity of the imidazole···HO—Ser residue (see Scheme 2). The fundamental difference with **10** is the prior formation of the alkoxide anion (generated with assistance from $Zn^{II}$, with a $pK_a$ of 7.4) before nucleophilic attack on the substrate. For the subsequent deacylation process, the $Zn^{II}$–$OH_2$ deprotonates with a $pK_a$ of approximately 7, and so the resulting $Zn^{II}$–$OH^-$ becomes an effective nucleophile.[21]

## Summary and Conclusions

The ethanol-pendant 1,5,9-triazacyclododecane ([12]ane$N_3$, $L_2$) forms a stable 1:1 complex **10** (or **20**) with $Zn^{II}$ at physiological pH, and the alcohol deprotonates with a $pK_a$ value of 7.4 to bind $Zn^{II}$ at the fourth coordination site at 25 °C, $I$ = 0.1 ($NaNO_3$), and [total zinc] = [total ligand] = 1 mM. This is a novel chemical model system which demonstrates that the serines at the active center of alkaline phosphatase can be deprotonated at physiological pH. The $Zn^{II}$-bound alkoxide anion in **10** is 4 times as strong a nucleophile toward 4-nitrophenyl acetate (NA) as the $Zn^{II}$-bound hydroxide in the [12]ane$N_3$ complex **7**. The activation parameters for these reactions suggest that the difference is mainly due to a more favorable "frequency factor" term for the reaction involving **10**. This is best explained by a smaller degree of solvation of the nucleophile in **10**, which therefore facilitates the attack at the electrophilic center of the substrate. We suspect that these facts may be relevant when considering the nucleophilic nature

(18) It is of interest to highlight a recent study on the active-site mutagenesis of alkaline phosphatase (produced by *Escherichia coli*) in ref 2c. A site-directed mutagenesis technique replaced Ser(102) with nonnucleophilic amino acids leucine and alanine. The removal of Ser(102) may open up a ligand site for water. Thus, a zinc-activated water is well positioned for a direct nucleophilic attack. These mutant enzymes still catalyze the hydrolysis of phosphate monoester with similar $K_m$ and $K_I$ (inorganic phosphate inhibition constant) values, although the $k_{cat}$ values are ca. 1/1000–1/500 smaller than that for the wild-type enzyme.

(19) In support of this interpretation, a recent X-ray study has shown that **7** readily precipitates from solution as a trimer with three intermolecular hydrogen bonds (i.e., $Zn^{II}$—$(HO^-)$···$HO^-$—$Zn^{II}$) and no intermolecular coordination bond between each $HO^-$ anion and any other $Zn^{II}$, suggesting the weaker nucleophilicity of the $HO^-$ anion (see ref 9a).

(20) (a) Bender, M. L.; Zerner, B. *J. Am. Chem. Soc.* **1961**, *83*, 2391. (b) Bender, M. L.; Zerner, B. *J. Am. Chem. Soc.* **1963**, *85*, 356. (c) Bruice, T. C.; Benkovic, S. *Bioorganic Mechanisms*; W. A. Benjamin: New York, 1966; Vol. 1, Chapter 2, p 212.

(21) Recently, an active-site mutagenesis of nonmetallo(serine enzyme β-lactamase was carried out to determine the role of Ser(68) at the active center. In this case, replacement of Ser(68) with glycine completely abolished the hydrolytic activity of the enzyme. See: Toth, M. J.; Murgola, E. J.; Schimmel, P. J. *J. Mol. Biol.* **1988**, *201*, 451.

of the alkoxide group at the active center of $Zn^{II}$ enzymes (e.g., alkaline phosphatase). Furthermore, in the course of NA hydrolysis by **10**, an "acetyl intermediate" **23** was generated in the rate-determining step, and its free ligand **24** was isolated for identification. Some of the properties of the acetyl intermediate are analogous to those of the acetyl intermediate **5** in chymotrypsin. Thus our $Zn^{II}$ alkoxide complex may offer a novel chemical model for various serine-involving enzymes. It is worth noting that in almost all of the previous model studies using cyclodextrins, etc., for serine enzymes,[22] NA hydrolysis was run in highly alkaline conditions (pH > 10) to generate the active nucleophilic alkoxide anions.

## Experimental Section

**General Information.** CHES (2-(cyclohexylamino)ethanesulfonic acid, Dojin Chemical) and the other reagents were of analytical grade from commercial sources and were used without further purification. IR and UV spectra were recorded on a Shimadzu FTIR-4200 and a Hitachi U-3200 spectrophotometer, respectively. Melting points were determined by a micro melting apparatus without any corrections. Conductance was measured with a TOA Conductivity Meter CM-20S and a TOA Conductivity Cell CG-511B. Elemental analysis was performed on a YANAKO CHN Corder MT-3. Thin-layer (TLC) and silica gel column chromatographies were performed on a Merck Art. 5554 (silica gel) TLC plate and on Wakogel C-300 silica gel, respectively.

**Synthesis of 1-(2-Hydroxyethyl)-1,5,9-triazacyclododecane ($L_2$)** (see Scheme III). To a solution of ethyl bromoacetate (4.1 g, 25 mmol) in 350 mL of $CHCl_3$ at 50 °C was added dropwise over 1 h a solution of 2,4-dioxo-1,5,9-triazacyclododecane (**11**)[13] (4.0 g, 20 mmol) and triethylamine (2.4 g, 24 mmol) in 150 mL of $CHCl_3$. The reaction mixture was then heated at reflux for 1 h. After the triethylamine hydrobromide was filtered off, the solvent was evaporated. The residue was dissolved in 100 mL of ethyl acetate and washed with water (50 mL × 4). The aqueous layer was then extracted with $CH_2Cl_2$ (70 mL × 3). The combined organic layers were dried over anhydrous $Na_2SO_4$. After evaporation of the solvent, the residue was recrystallized from 5 mL of ethyl acetate to obtain **12** as colorless needles (3.6 g, 62% yield), mp 97.0–98.0 °C. IR (KBr pellet): 3330, 2984, 2872, 1740, 1669, 1632, 1564, 1537, 1468, 1294, 1202, 1159, 1090, 1063, 1036, 988, 959, 874, 721, 606 $cm^{-1}$. TLC (eluent $CH_2Cl_2$/MeOH, 20:1) $R_f$ = 0.24. $^1H$ NMR ($CDCl_3$): δ 1.32 (3 H, t, $J$ = 7.1 Hz, $CH_3$), 1.63–1.69 (4 H, m, $CCH_2C$), 2.58–2.62 (4 H, m, $NCH_2$), 3.17 (2 H, s, $COCH_2CO$), 3.28 (2 H, s, $NCH_2CO$), 3.40–3.45 (4 H, m, $NCH_2$), 4.26 (2 H, q, $J$ = 7.1 Hz, $COOCH_2$), 8.33 (2 H, b, CONH). Anal. Calcd for $C_{13}H_{23}N_3O_4$: C, 54.7; H, 8.1; N, 14.7. Found: C, 54.6; H, 8.2; N, 14.6.

The dioxo macrocycle **12** (1.5 g, 5.3 mmol) was added to a solution of freshly distilled $BH_3$–THF complex[13] in 250 mL of dry THF at 0 °C. The solution was stirred at room temperature for 1 h and then heated at 60 °C for 1 day. After decomposition of the excess amount of the hydroborane complex with water at 0 °C, the solvent was evaporated. The residue was dissolved in 100 mL of 3 M aqueous HCl, and then the solution was heated at 80 °C for 2 h. After evaporation of the solvent, the residue was passed through an anion-exchange column of Amberlite IRA-400 with water to obtain $L_2$ as a colorless oil. Crystallization of the oil from 48% aqueous HBr–MeOH afforded colorless prisms as a tribromide salt ($L_2$·3HBr) in 58% yield (1.40 g), mp 220 °C dec. IR (KBr pellet): 3320, 2950, 2737, 1590, 1580, 1480, 1456, 1036 $cm^{-1}$. $^1H$ NMR ($D_2O$, pD 6.3): δ 2.03 (4 H, quintet, $J$ = 5.6 Hz, $CCH_2C$), 2.06–2.24 (2 H, m, $CCH_2C$), 2.79 (2 H, t, $J$ = 5.3 Hz, $NCH_2C$), 2.92 (4 H, t, $J$ = 5.8 Hz, $NCH_2$), 3.48–3.26 (8 H, m, $NCH_2$), 3.87 (2 H, t, $J$ = 5.3 Hz, $CH_2O$). $^{13}C$ NMR ($D_2O$, pD 6.3): δ 23.8, 24.2, 47.1, 48.7, 55.6, 55.8, 59.8. Anal. Calcd for $C_{11}H_{28}N_3O_1Br_3$: C, 28.8; H, 6.2; N, 9.2. Found: C, 29.1; H, 6.3; N, 9.2.

**Synthesis of 1-(3-Hydroxypropyl)-1,5,9-triazacyclododecane ($L_3$).** A solution of **8** (0.88 g, 4.4 mmol) in 50 mL of methyl acrylate **13** was heated at reflux in the dark for 1 day. After evaporation of the unreacting **13**, the residue was recrystallized from EtOAc to give 9-(2-(methoxycarbonyl)ethyl)-2,4-dioxo-1,5,9-triazacyclododecane (**15**) as colorless prisms (1.05 g, 83% yield), mp 124.0 °C. IR (KBr pellet): 3301, 2955, 2942, 1738, 1644, 1559, 1536, 1440, 1381, 1318, 1287, 1215, 1194, 1180, 1150, 1084, 1040, 951, 721, 610 $cm^{-1}$. $^1H$ NMR ($CDCl_3$): δ 1.71–1.77 (4 H, m, $CCH_2C$), 2.47–2.49 (4 H, m, $CH_2N$), 2.56–2.60 (2 H, m, $CCH_2CO$), 2.64–2.67 (2 H, m, $CH_2N$), 3.15 (2 H, s, $COCH_2CO$), 3.38–3.42 (4 H, m, $CONCH_2$), 3.71 (3 H, s, $CH_3$), 7.69 (2 H, b, CONH). $^{13}C$ NMR ($CDCl_3$): δ 174.7, 167.3, 55.8, 52.2, 49.8, 46.3, 41.0, 32.7, 24.5. Anal. Calcd for $C_{13}H_{23}N_3O_4$: C, 54.7; H, 8.1; N, 14.7. Found: C, 54.8; H, 8.2; N, 14.6.

Synthesis of $L_3$·3HBr from the dioxo macrocycle **15** was similar to that of $L_2$·3HBr (24% yield), mp 204.0 °C dec. IR (KBr pellet): 3378, 2986, 2824, 2718, 1609, 1586, 1487, 1435, 1379, 1358, 1071, 1057, 1030 $cm^{-1}$. $^1H$ NMR ($D_2O$, pD 3): δ 1.96–2.04 (2 H, m, $CCH_2CO$), 2.19–2.29 (6 H, m, $CCH_2C$), 3.31–3.38 (10 H, m, $CH_2N$), 3.43–3.51 (4 H, m, $CH_2N$), 3.72 (2 H, t, $J$ = 5.9 Hz, $CH_2O$). $^{13}C$ NMR ($D_2O$, pD 3): δ 61.8, 55.9, 50.7, 45.2, 44.6, 29.0, 23.6, 20.9. Anal. Calcd for $C_{12}H_{27}N_3O$·3HBr: C, 30.9; H, 6.8; N, 8.4. Found: C, 30.5; H, 6.4; N, 8.9.

**Synthesis of 1-(3-Hydroxybutyl)-1,5,9-triazacyclododecane ($L_4$).** A solution of **8** (2.0 g, 10 mmol) in 25 mL of methyl vinyl ketone **14** was heated at reflux in the dark for 1 day. After evaporation of the remaining **14**, the residue was recrystallized from $CH_3CN$ to give 9-(3-oxobutyl)-2,4-dioxo-1,5,9-triazacyclododecane (**16**), as colorless needles (2.34 g, 87% yield), mp 131.0 °C. IR (KBr pellet): 3320, 2936, 2843, 1705, 1668, 1638, 1559, 1536, 1449, 1397, 1372, 1356, 1304, 1265, 1252, 1223, 1173, 1146, 1092, 1055, 986, 950, 872, 700, 586 $cm^{-1}$. $^1H$ NMR ($CDCl_3$): δ 1.76 (4H, m, $CCH_2C$), 2.22 (3 H, s, $CH_3$), 2.46 (4 H, t, $J$ = 5.2 Hz, $NCH_2$), 2.46 (2 H, t, $J$ = 5.5 Hz, $CCH_2CO$), 2.72 (2 H, t, $J$ = 5.5 Hz, $NCH_2C$), 3.08 (2 H, s, $COCH_2CO$), 3.39 (4 H, m, $CONCH_2$), 7.67 (2 H, b, CONH). Anal. Calcd for $C_{13}H_{23}N_3O_3$: C, 58.0; H, 8.6; N, 15.6. Found: C, 57.9; H, 8.8; N, 15.8.

The synthesis of $L_4$·3HBr from the dioxo macrocycle **16** was similar to that of $L_2$·3HBr (56% yield), mp 215 °C dec. IR (KBr pellet): 3141, 2955, 2797, 2674, 1591, 1478, 1454, 1362, 1148, 1065, 855, 739 $cm^{-1}$. $^1H$ NMR ($D_2O$, pD 6): 1.25 (3 H, d, $J$ = 6.4 Hz, $CH_3$), 1.80–1.87 (2 H, m, $CCH_2CO$), 1.97 (2 H, quintet, $J$ = 5.5 Hz, $CCH_2C$), 2.02–2.10 (4 H, m, $CCH_2C$), 3.02–3.31 (14 H, m, $NCH_2$), 3.93–4.02 (1 H, m, CCHOC). $^{13}C$ NMR ($D_2O$, pD 6): δ 23.8, 24.6, 25.1, 32.9, 47.3, 49.3, 52.1, 53.4, 69.0. Anal. Calcd for $C_{13}H_{32}N_3O_1Br_3$: C, 32.1; H, 6.6; N, 8.6. Found: C, 32.5; H, 6.7; N, 8.6.

**Synthesis of Dimeric Zinc(II) Complexes with $L_2$, 17·$(ClO_4)_2$ and 17·$(PF_6)_2$.** $Zn(ClO_4)_2$·$6H_2O$ (372 mg, 1.0 mmol) was dissolved in an aqueous solution (4 mL) of $L_2$·3HBr (458 mg, 1.0 mmol). The solution pH was adjusted to 9 with 1 M NaOH aqueous solution and then a solution (1 mL) of 1 M $NaClO_4$ was added. Colorless prisms of 17·$(ClO_4)_2$ were obtained by slow evaporation in 62% yield. IR (KBr pellet): 3282, 2926, 2855, 1462, 1373, 1360, 1281, 1246, 1120, 1100, 1084, 909, 625, 486 $cm^{-1}$. $^1H$ NMR ($D_2O$): δ 1.69 (1 H, dtt, $J$ = 16, 7, 2 Hz, H($C_7$)), 1.70–1.81 (2 H, m, H($C_{3,11}$)) 1.91–2.10 (2 H, m, H($C_{3,11}$)), 2.14 (1 H, dtt, $J$ = 16, 10, 2 Hz, H($C_7$)), 2.68 (2 H, t, $J$ = 5 Hz, H($C_{13}$)), 2.89 (2 H, ddd, $J$ = 14, 7, 2 Hz, H($C_{6,8}$)), 2.96 (2 H, ddd, $J$ = 14, 9, 2 Hz, H($C_{4,10}$)), 2.90–3.00 (4 H, m, H($C_{2,12}$)), 3.16 (2 H, ddd, $J$ = 14, 8, 2 Hz, H($C_{4,10}$)), 3.23 (2 H, ddd, $J$ = 14, 10, 2 Hz, H($C_{6,8}$)), 3.71 (2 H, t, $J$ = 5 Hz, H($C_{14}$)). $^1H$ NMR ($CD_3CN$): δ 1.66 (1 H, dtt, $J$ = 16, 7, 2 Hz, H($C_7$)), 1.72–1.81 (2 H, m, H($C_{3,11}$)), 1.88–1.99 (2 H, m, H($C_{3,11}$)), 2.04 (1 H, dtt, $J$ = 16, 8, 2 Hz, H($C_7$)), 2.53 (2 H, t, $J$ = 7 Hz, H($C_{13}$)), 2.78–2.89 (2 H, m, H($C_{4,6,8,10}$)), 2.78 (4 H, t, $J$ = 6 Hz, H($C_{2,12}$)), 3.06–3.18 (2 H, m, H($C_{4,6,8,10}$)), 3.58 (2 H, b, HN), 3.74 (2 H, t, $J$ = 7 Hz, H($C_{14}$)). $^{13}C$ NMR ($D_2O$): δ 26.5, 27.5, 53.2, 53.7, 60.4, 60.7, 62.4. $^{13}C$ NMR ($CD_3CN$): δ 24.3, 25.5, 50.7, 51.1, 57.3, 59.2, 60.6. Anal. Calcd for $C_{11}H_{24}N_3O_5Cl_1Zn$: C, 34.8; H, 6.4; N, 11.1. Found: C, 34.9; H, 6.3; N, 11.1.

$L_2$·3HBr (400 mg, 0.87 mmol) was passed through an anion-exchange column of Amberlite IRA-400 with water. After the solvent was evaporated, 2 mL of an aqueous solution of $ZnBr_2$ (200 mg, 0.89 mmol) was added to the residue, and the solution pH was adjusted to 9 with 1 M NaOH aqueous solution. After filtration, 5 mL of a $KPF_6$ (803 mg, 4.4 mmol) aqueous solution was added. Colorless needles of 17·$(PF_6)_2$ were obtained in 88% yield. NMR data are the same as those for 17·$(ClO_4)_2$. IR (KBr pellet): 3301, 2934, 2865, 1466, 1377, 1364, 1306, 1281, 1246, 1157, 1115, 1100, 1082, 1067, 1032, 903, 843, 741, 602, 557 $cm^{-1}$. Anal. Calcd for $C_{11}H_{24}N_3OF_6PZn$: C, 31.1; H, 5.7; N, 9.9. Found: C, 31.1; H, 5.7; N, 9.8.

**Isolation of 1-(2-Acetoxyethyl)-1,5,9-triazacyclododecane (24).** Because the lifetime of the acetate intermediate **23** was too short to permit its isolation from an aqueous buffer solution (pH 9), a nonbuffer solution was used to prevent the following intramolecular acetate hydrolysis. 17·$(PF_6)_2$ (76 mg, 0.18 mmol) and 4-nitrophenyl acetate (38 mg, 0.21 mmol) were dissolved in 5 mL of $CH_3CN$ and stirred at room temperature

(22) (a) Tee, O. S.; Bozzi, M.; Hoeven, J. J.; Gadosy, T. A. *J. Am. Chem. Soc.* **1993**, *115*, 8990. (b) Hengge, A. C.; Cleland, W. W. *J. Org. Chem.* **1991**, *56*, 1972.

for 2 h. After evaporation of the solvent, an aqueous solution (10 mL) of EDTA (0.33 g, 0.89 mmol) and $KPF_6$ (98 mg, 0.53 mmol) was added to the residue. The solution pH was adjusted to 9 with 1 M NaOH aqueous solution, and then the solution was extracted with $CH_2Cl_2$ (10 mL × 3). After the organic solvent was evaporated, the residue was dissolved in 1 mL of $CH_2Cl_2$, and then 5 mL of ether was added to obtain colorless crystals of **24**·$HPF_6$ (52 mg, 73% yield), mp 108.0 °C. IR (KBr pellet): 3430, 3374, 2969, 2832, 1736, 1476, 1379, 1275, 1250, 1051, 978, 842, 557 $cm^{-1}$. TLC (eluent $CH_2Cl_2$/MeOH, 20:1) $R_f$ = 0.39. $^1H$ NMR ($CD_3CN$): δ 1.66–1.75 (6 H, m, $CCH_2C$), 2.14 (3 H, s, $CCH_3$), 2.60 (4 H, t, $J$ = 5.8 Hz, $NCH_2C$), 2.65 (2 H, t, $J$ = 5.7 Hz, $NCH_2C$), 2.81 (4 H, t, $J$ = 5.3 Hz, $NCH_2C$), 2.97 (4 H, t, $J$ = 5.4 Hz, $NCH_2C$), 4.19 (2 H, t, $J$ = 5.6 Hz, $OCH_2C$). Anal. Calcd for $C_{13}H_{28}N_3O_2PF_6$: C, 38.7; H, 7.0; N, 10.4. Found: C, 38.9; H, 7.1; N, 10.6.

**Crystallographic Study.** A colorless crystal with dimensions 0.2 × 0.15 × 0.05 mm of **17**·$(ClO_4)_2$ was used for data collection. The lattice parameters and intensity data were measured on a Rigaku AFC5R diffractometer with graphite-monochromated Cu Kα radiation and a 12-kW rotating anode generator. The structure was solved by direct methods, and the non-hydrogen atoms were refined either anisotropically or isotropically. The final cycle of full-matrix least-squares refinement was based on 1765 observed reflections to give $R$ = 0.071 and $R_w$ = 0.099. All calculations were performed using the TEXSAN crystallographic software package developed by Molecular Structure Corporation (1985). Drawing of an ORTEP structure of **17** and the structure determination of **18** (by MM2 method) were carried out with the computer graphic system CAChe (Sony Tektronics Co.).

**Potentiometric pH Titrations.** The preparation of the test solutions and the calibration of the electrode system were described earlier.[9a] All test solutions (50 mL) were kept under argon (>99.999% purity) atmosphere at 15.0, 25.0, and 35.0 ± 0.1 °C. The potentiometric pH titrations were carried out at [total ligand] = 0.5, 1, and 2 mM in the presence or absence of equimolar $ZnSO_4$ at $I$ = 0.10 ($NaNO_3$), where at least three independent titrations were always made. The calculation methods for ligand protonation constants ($K_n$) and two $Zn^{II}$ complexation constants ($K$(ZnL) and $K_a$) were the same as described previously,[9a] where computer program written in Microsoft BASIC was used (presented as supplementary material). Finally, the computer program BEST[23] was used for determination of $K_n$, $K$(ZnL), $K_a$, and the dimer formation constant $K_d$ and for calculation of a distribution diagram for relative species concentration as a function of −log [$H^+$]. The protonation constants $K_n$ are defined as $[H_nL]/[H_{n-1}L]a_{H^+}$, the 1:1 metal complexation constant $K$(ZnL) as $[ZnL]/[Zn^{II}][L]$, the deprotonation constant $K_a$ as $[ZnH_{-1}L]a_{H^+}/[ZnL]$, and the dimerization constant $K_d$ as $[(ZnH_{-1}L)_2]/[ZnH_{-1}L]^2$. The large confidence limit (±0.3) of log $K_d$ values for the dimeric complex **17** is due to its small contribution to the pH titration data. The values used of $K_w'$ (=$[H^+][OH^-]$) and $f_{H^+}$ at 15, 25, and 35 °C were $10^{-14.15}$, $10^{-13.79}$, and $10^{-13.48}$ and 0.827, 0.825, and 0.823, respectively.

**NMR Study.** $^1H$ (400 MHz) and $^{13}C$ (100 MHz) NMR spectra were recorded on a JEOL α-400 spectrometer. 3-(Trimethylsilyl)propionic-2,2,3,3-$d_4$ acid sodium salt (Merck) in $D_2O$ and tetramethylsilane (Merck) in organic solvents were used as internal references for $^1H$ and $^{13}C$ NMR measurements. Solutions of $ZnH_{-1}L_2$ in $D_2O$ (99.9 atom % D from Aldrich) and in $CD_3CN$ (100 atom % D from Aldrich) were subjected to $^1H$ NMR at a constant temperature (25–40 °C), where the total $Zn^{II}$ concentration is 0.5, 1.0, 2.5, 10, or 20 mM. Peak assignments for the $Zn^{II}$ complexes were made on the basis of COSY and differential NOE spectroscopies at [total zinc] = [total ligand] = 20 mM and 30 °C.

**Kinetics. 4-Nitrophenyl Acetate Hydrolysis Catalyzed by 10.** The hydrolysis (or 4-nitrophenolate release reaction) rate of 4-nitrophenyl acetate (NA) was measured by an initial slope method (following the increase in 400-nm absorption of released 4-nitrophenolate) in 10% (v/v) $CH_3CN$ aqueous solution at 15.0, 25.0, and 35.0 ± 0.5 °C, as previously described for **7**-catalyzed NA hydrolysis.[8a] Buffered solutions containing 20 mM CHES buffer (pH 9.5, 9.3, and 9.1, respectively) were used, and the ionic strength was adjusted to 0.10 with $NaNO_3$ (ca. 90 mM). For the initial rate determination, the following procedure was employed. NA (0.1, 0.5, 1.0, and 2.0 mM) and **10** (0.5, 1.0, 2.0, and 3.0 mM) were mixed in the buffered solution, and the UV absorption increase was recorded immediately and then followed generally until ca. 2% formation of 4-nitrophenolate, where log ε of 4-nitrophenolate was 4.24 at 400 nm. The observed rate constants $k_{obs}$ ($s^{-1}$) were calculated from the decay slope. All experiments were run in triplicate, and tabulated data represent the average of these experiments. Rate constants were reproducible to ±5%. To check if the NA hydrolysis was recyclic, we followed the NA hydrolysis rate until 80% completion at [NA] = 1.0 mM and [**10**] = 0.50 mM using the absorption increase at 458 nm (log ε 3.18). Under these conditions, ca. 0.5 mM and ca. 0.3 mM NA were hydrolyzed by **10** and the buffer alone, respectively. The second-order rate constant for **10** was identical to the initial rate constant determined above.

**Acknowledgment.** E.K. is thankful to the Ministry of Education, Science and Culture in Japan for the financial support by a Grant-in-Aid for Scientific Research on Priority Areas "Bioinorganic Chemistry" (No. 03241105) and for Scientific Research (A) (No. 04403024). T.K. is thankful to the Ministry of Education, Science and Culture in Japan for the financial support by a Grant-in-Aid for Encouragement of Young Scientists (No. 05857265). NMR instruments and a computer graphic system (CAChe produced by Tektronix Co.) in the Medical Molecules Exploring Center (MMEC) of Hiroshima University were used.

**Supplementary Material Available:** Tables of atomic coordinates, equivalent isotropic temperature factors, and anisotropic temperature factors for **17**·$(ClO_4)_2$; calculation strategy for the preliminary $K$(ZnL) and p$K_a$ values with a list of the software (8 pages); listing of observed and calculated structure factors for **17**·$(ClO_4)_2$ (12 pages). This material is contained in many libraries on microfiche, immediately follows this article in the microfilm version of the journal, and can be ordered from the ACS; see any current masthead page for ordering information.

(23) Martell, A. E.; Motekaitis, R. J. *Determination and Use of Stability Constants*, 2nd ed.; VCH: New York, 1992.